7-1985

The Frontal Hydraulic Head: A Micro-α Scale (~1 km) Triggering Mechanism for Mesoconvective Weather Systems

M. A. Shapiro
National Oceanic and Atmospheric Administration

Tamara Hampel
National Oceanic and Atmospheric Administration

Doris Rotzoll
University of Wisconsin-Madison

F. Mosher
University of Wisconsin-Madison, moshe774@erau.edu

The Frontal Hydraulic Head: A Micro-α Scale (~1 km) Triggering Mechanism for Mesoconvective Weather Systems

M. A. SHAPIRO AND TAMARA HAMPEL

NOAA/ERL/Wave Propagation Laboratory, Boulder, CO 80303

DORIS ROTZOLL AND F. MOSHER

Space Science and Engineering Center, University of Wisconsin, Madison, WI 53706

(Manuscript received 9 October 1984, in final form 12 March 1985)

ABSTRACT

Measurements from the NOAA Boulder Atmospheric Observatory (BAO) 300 m tower, the National Center for Atmospheric Research (NCAR) Sabreliner aircraft, and the NOAA GOES-5 satellite, give evidence for the cross-front scale collapse of nonprecipitating surface cold-frontal zones to horizontal distances of ~1 km or less. The leading edges of these fronts possess the characteristic structure of density current flows: an elevated hydraulic head followed by a turbulent wake. Vertical motions at the frontal heads exceed 5 m s^{-1} at 300 m (AGL). The ascent at the frontal head may act as a (~1 km-scale) triggering mechanism for the release of potential instability and the formation of intense squall-line mesoconvection.

1. Introduction

In reviewing the concepts and analyses of surface fronts, one finds that fronts near the ground were first considered zero-order discontinuities in density (temperature) and wind velocity, between air masses of different origin. The early observational studies (reviewed by Bergeron, 1959) documented the abrupt switch in wind direction and temperature drop during frontal passage. The accompanying theoretical treatments (e.g., Margules, 1906) used laws of hydrodynamics applied to "two-density" fluid models containing a sloping frontal interface in describing the motion, slope and vertical circulations of fronts. With the advent of kite and balloon-borne upper-air observations, it was discovered that fronts aloft were actually transition zones of finite width having characteristic vertical and horizontal scales of ~1 km and 100 km respectively (Bjerknes and Palmén, 1937). At this stage in frontal history, the concept of zero-order discontinuities at fronts within synoptic-scale (~1000 km) cyclones was discarded, and fronts were thereafter treated as sloping transition zones bounded by first-order discontinuities in temperature and velocity. However, it was recognized that sharp horizontal discontinuities could exist at the micro-α scale (0.2–2 km) such as at the outflow boundaries of convective precipitation systems, land–sea breeze convergences and orographically forced flows (Charba, 1974; Goff, 1976; Simpson *et al.*, 1977; Matthews, 1981; Wakimoto, 1982; Carbone, 1982; and Hobbs and Perrson, 1982).

It is the authors' opinion that the shift from the discontinuous wedge (two-density) model to the continuous "zone" model was the result of combining synoptically spaced (~400 km) upper-air observations with the meso-β scale spacing (~100 km) of the hourly reporting surface stations, and the decline in the use of single-station (continuous record) analysis of frontal zones. Furthermore, with the expansion of synoptic observing networks and the application of the Norwegian cyclone-frontal models, fronts were treated as synoptic-scale (~1000 km) in length whose narrow width resulted from the contractions of synoptic thermal gradients by the geostrophic deformations and their ageostrophic circulation response. The quasi- and semi-geostrophic equations which were later used to describe frontal contractions did not contain the nonhydrostatic physics which contribute to the final frontal scale collapse of the earlier wedge model or sharp discontinuities which had been observed with continuous temporal resolution observations.

Bergeron (1928) first described the role of synoptic-scale deformation fields in the contraction of temperature and velocity gradients into meso-β scale (~100 km) frontal zones. Since then, the importance of geostrophic deformations and their coupled vertical secondary circulations have been examined in frontal studies by Petterssen (1956), Sawyer (1956), Eliassen (1959, 1962), Williams (1967), Hoskins and Bretherton (1972), and Shapiro (1981), among others. Eliassen (1959) recognized that secondary circulations act as a "selfsharpening" process to accelerate the

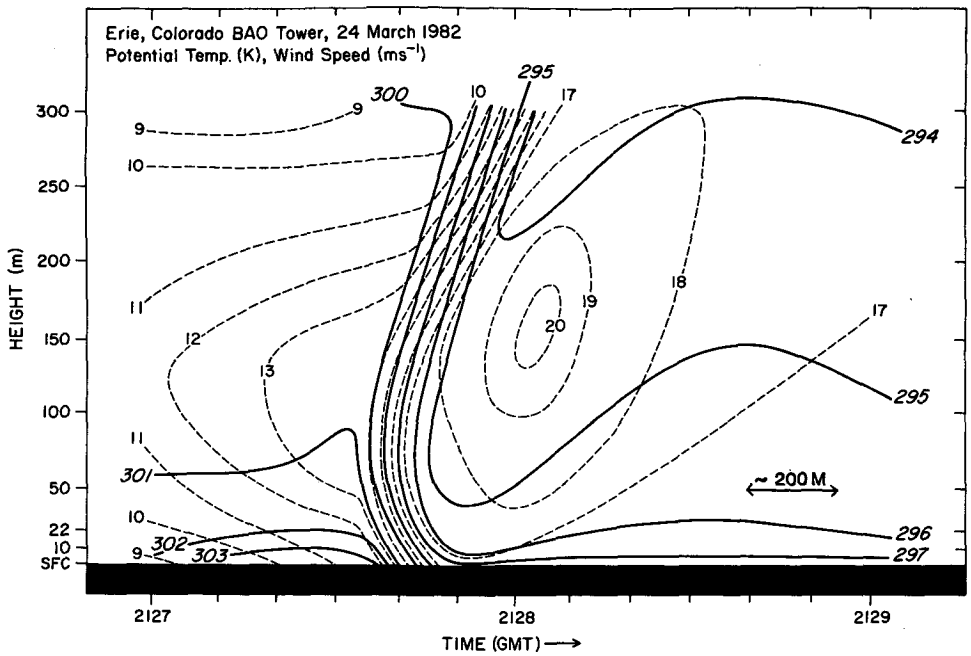

FIG. 1. Time–height section analysis of potential temperature (K, solid lines) and front-normal horizontal (positive toward the warm air) wind component (m s^{-1}, dashed lines) for a surface cold front passage at the Boulder Atmospheric Observatory 300 m tower, 24 March 1982 (from Shapiro, 1984).

scale contraction of surface fronts. Williams (1967) and Hoskins and Bretherton (1972) simulated this process (ageostrophic contraction) through numerical and analytic solutions, respectively. In the absence of fine-scale turbulent motions, there are no limits to the scale to which frontal gradients may contract

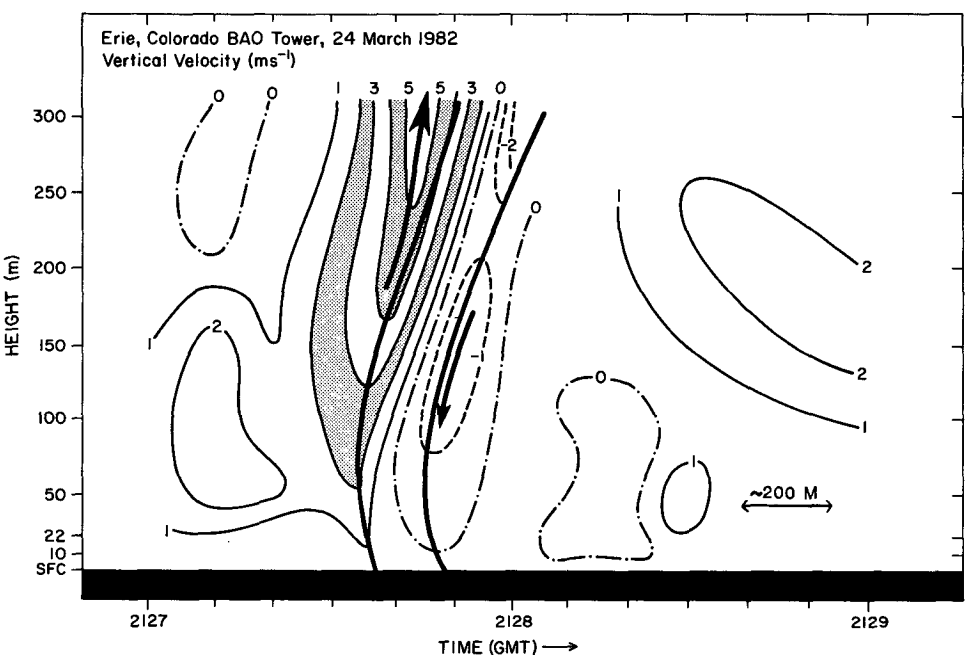

FIG. 2. Cross section of vertical motion (m s^{-1}) for Fig. 1. Frontal boundaries, heavy solid lines (from Shapiro, 1984).

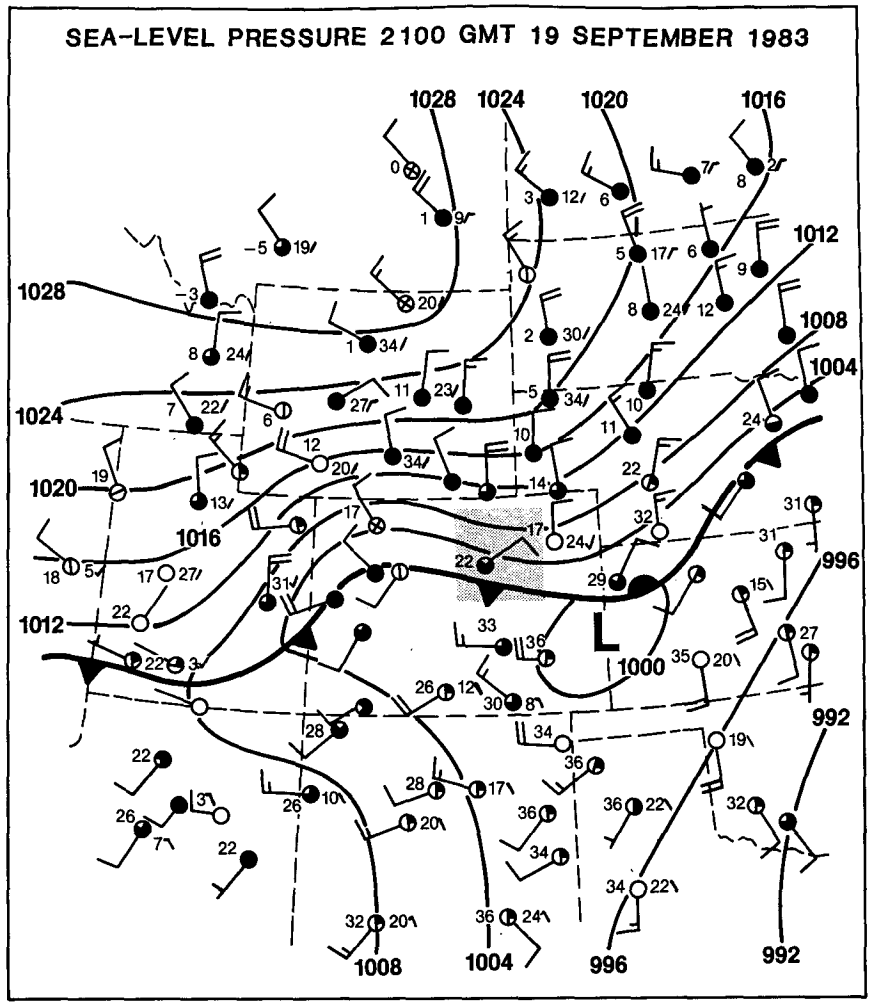

FIG. 3. National Weather Service sea-level pressure (mb) analysis and frontal analysis at 2100 GMT 19 September 1983. Surface wind vectors full barb = 5 m s^{-1}; half barb = 2.5 m s^{-1}. Surface temperature (°C) and 3 h pressure tendency, plotted at stations. Cloud cover (octants), are shown within station circle. Area of PROFS surface mesonetwork (Fig. 4) indicated as shaded area in northeastern Colorado.

under the combined actions of geostrophic and ageostrophic motion. Inviscid, adiabatic frontogenesis produces infinitesimally narrow fronts within a finite time (Hoskins and Bretherton, 1972). The finite scale of frontal zones is a balance between frontogenetical synoptic-scale forcing and frontolytical turbulent-scale mixing. Further frontal contractions occur when moist convection breaks out within the ascending motion at the leading edge of fronts (e.g., Newton, 1950; Carbone, 1982), after the frontal dynamics are modified by the effects of water vapor phase changes and nonhydrostatic pressure changes. Surface boundary layer heat and momentum fluxes also contribute to vertical circulations about fronts (e.g., Keyser and Anthes, 1982; Shapiro, 1982; Koch, 1984). In summary, a wealth of information and considerable understanding has been acquired about the structure and processes which govern the evolution of surface fronts. One can say that surface fronts are presently considered one of the better understood and predictable of mesoscale atmospheric phenomena.

The present study was inspired by observations from the 300 m meteorological tower of the NOAA/Wave Propagation Laboratory (WPL) Boulder Atmospheric Observatory (BAO), which documented the micro-α scale contraction of a nonprecipitating surface cold front to a horizontal cross-front distance of less than 200 m (Shapiro, 1984). Vertical motions and cross-front convergence were found to be two orders of magnitude larger than previously observed for "typical" cold fronts, such as shown in Sanders (1955). Figure 1 shows the potential temperature and

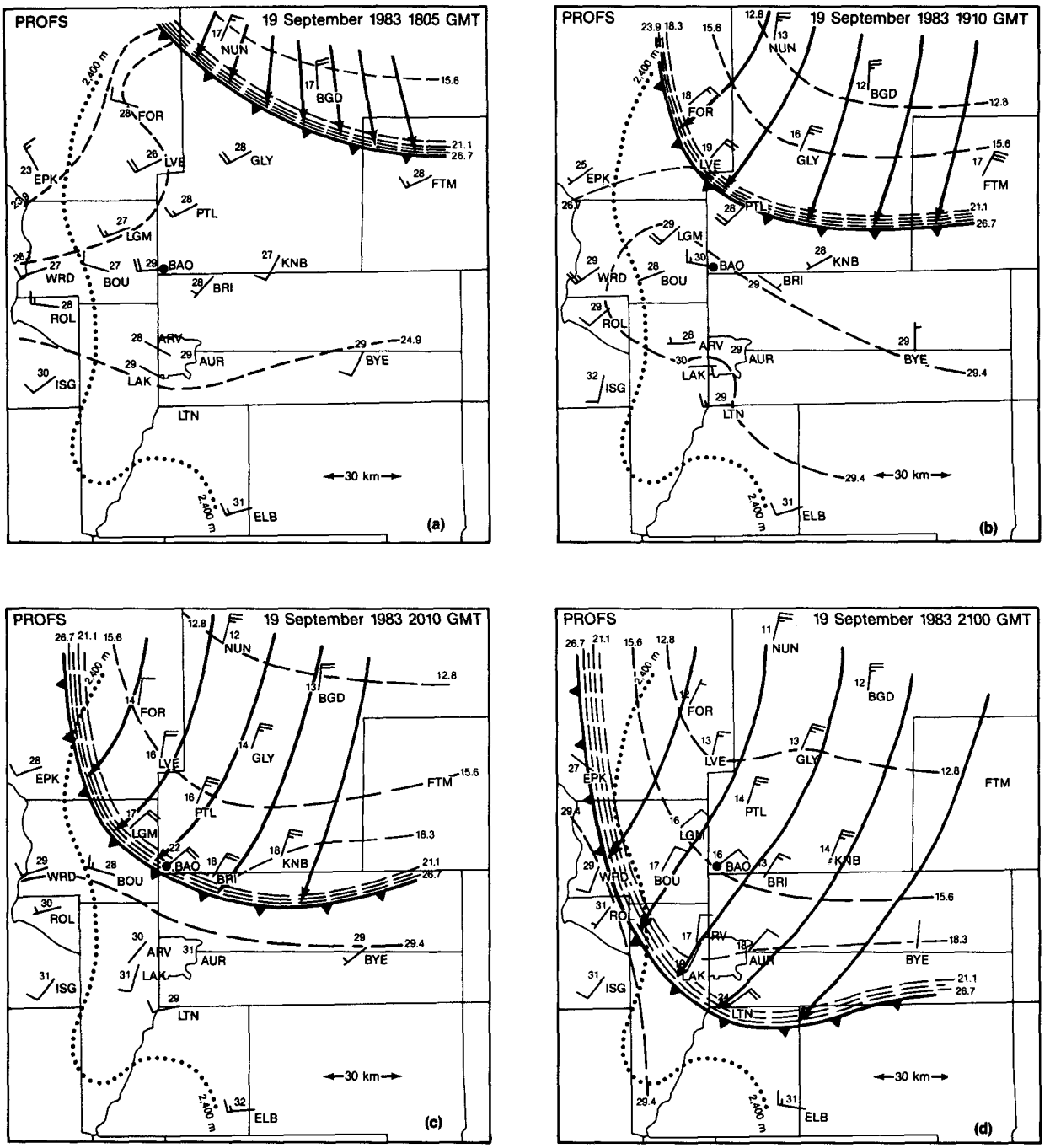

FIG. 4. Surface potential temperature, using a reference level of 850 mb, °C, (dashed lines) and streamlines (solid lines) at (a) 1805 GMT, (b) 1910 GMT, (c) 2010 GMT and (d) 2100 GMT 19 September 1983 from the PROFS surface mesonetwork. Location of BAO tower, black dot; 2400 m topographic height contour, dotted line. Wind vectors, as in Fig. 3.

cross-front wind speed, and Fig. 2 shows the vertical motion for this case.

In the present study, we provide additional documentation of this fine-scale structure. The first example is another case observed at the BAO tower. The second is a sharp cold front documented with the NCAR Sabreliner research aircraft over west Texas. In both cases, the width of the front was ~1 km near the ground and the leading edge of the front had an elevated "head" similar in form to that

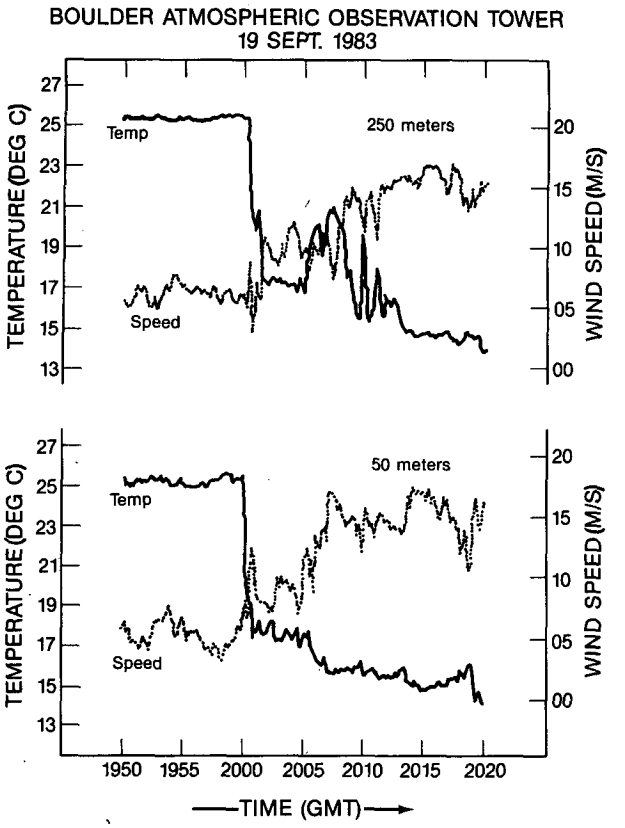

FIG. 5. Temperature (°C, solid lines) and wind speed (m s^{-1}, dotted lines) for 1950 to 2020 GMT 19 September 1983, measured at the 250 m level (top) and 50 m level of the BAO tower.

described for density current flows (Schmidt, 1913; Middleton, 1966; Simpson, 1969, 1972; and a summary by Fultz, 1951). This structure is similar to that found at the leading edge of thunderstorm outflows (Charba, 1974; Goff, 1976; Matthews, 1981) and their numerical simulation (Mitchell and Hovermale, 1977). The third example is based solely on the analysis of conventional surface observations and satellite cloud images.

The uniqueness of the present study lies in its documentation of the elevated head structure at nonprecipitating, synoptically forced surface fronts. The fronts described herein are shown to have collapsed to such a fine horizontal scale that nonhydrostatic pressure forces contribute to the formation of a density current "head" at their leading edge. The significance of this finding is that the large ascending motions (~5 m s^{-1}) at the frontal head may trigger mesoconvective weather systems, when the frontal head propagates into a region of potentially unstable air. This suggested triggering mechanism is similar to the hydraulic pressure jump mechanism previously described (but not widely acclaimed) in earlier studies by Freeman (1948), Abdullah (1949) and Tepper (1950).

2. Instrumentation

The observations for this study were taken with a variety of observing systems. Surface temperature and wind velocity were obtained from the NOAA Program for Regional Observing and Forecasting Services (PROFS) mesoscale network located east of the Rocky Mountains near Denver, Colorado. At the center of the network (30 km north of Denver), the BAO tower (Kaimal and Gaynor, 1983) provided fast-response (<1 s) measurements of horizontal velocity, vertical velocity and temperature at eight levels (10, 22, 50, 100, 150, 200, 250 and 300 m). The NOAA/WPL acoustic sounder (Brown and Hall, 1978) profiles (adjacent to the tower) were a source of additional information during frontal passage. The National Center for Atmospheric Research (NCAR) Sabreliner research aircraft provided 1 s measurements of horizontal wind velocity, vertical motion, pressure, temperature and moisture during frontal penetration over west Texas. Satellite visible imagery of narrow (rope-like) cloud lines and of mesoconvective cloud systems,

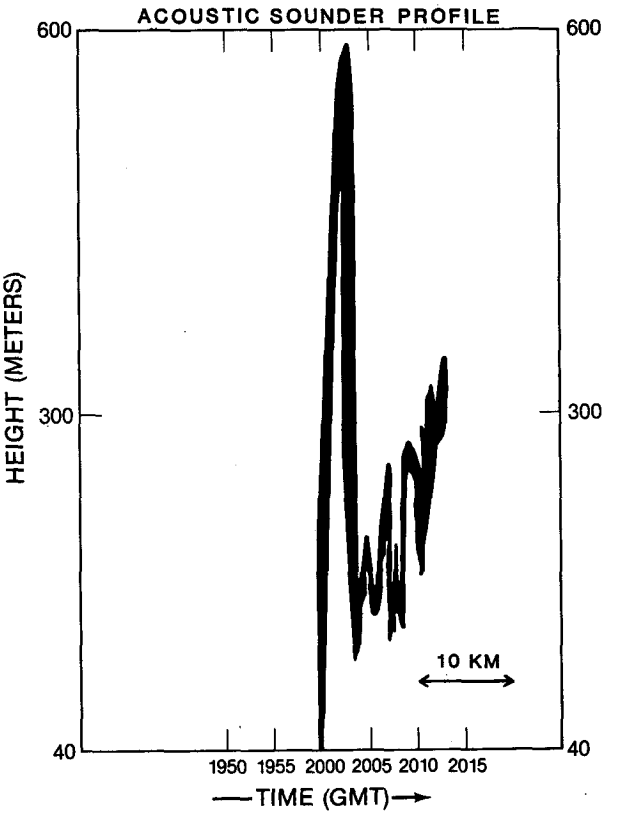

FIG. 6. Acoustic sounder record of the frontal passage for 1950 to 2015 GMT 19 September 1983, measured at the BAO tower.

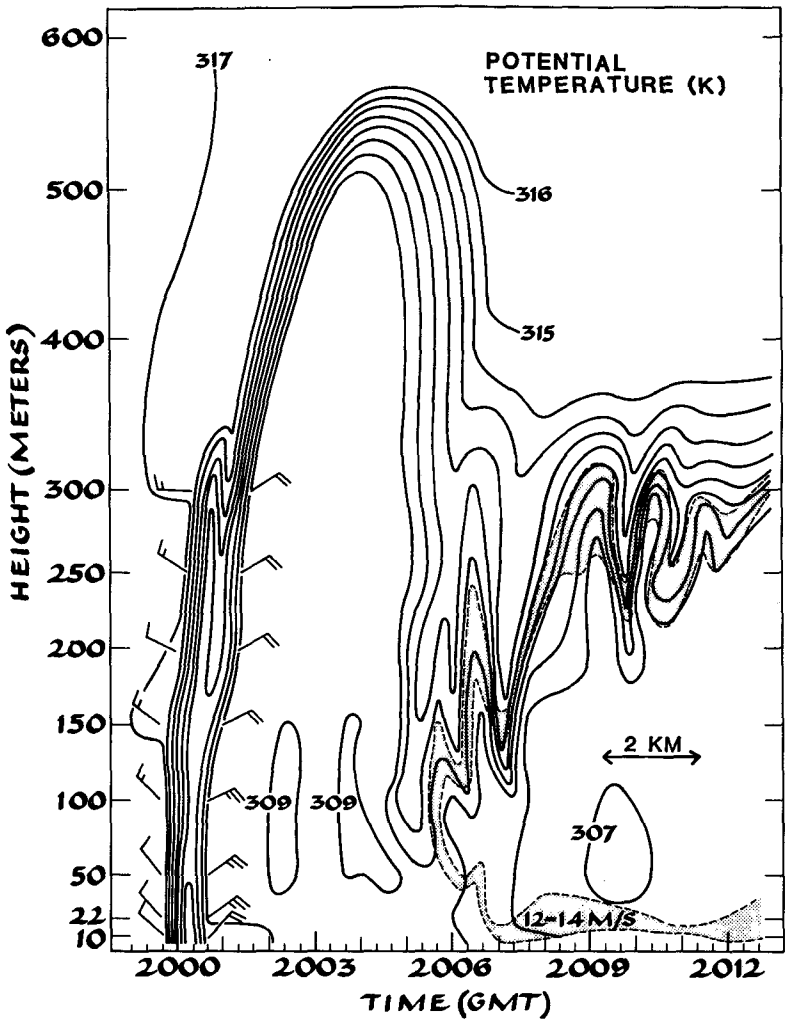

FIG. 7. Frontal passage at the BAO tower for 1959 to 2013 GMT 19 September 1983. Analysis of potential temperature (K, solid lines) derived from tower data up to 300 m and the acoustic record (Fig. 6) between 300 and 600 m. Region of the 12–14 m s^{-1} wind speed surge, stippled area; tower wind vectors preceding and following the passage of the front, wind barbs as in Fig. 3.

were obtained from special processing of NOAA/GOES-5 satellite images with the University of Wisconsin, McIDAS System. Satellite infrared images were obtained with the NOAA/Environmental Research Group ground station receiver.

3. The surface cold front of 19–20 September 1983

On 19 September 1983, a sharp cold front moved southward through eastern Colorado in advance of the first major Canadian outbreak of late summer. A synoptic view at 2100 GMT 19 September (Fig. 3) showed the front oriented east–west across Colorado. Temperatures in advance of the front exceeded 30°C, while to the north they were near 0°C. A mesoscale view of the front was observed by the PROFS surface network (Fig. 4). The station temperatures (Fig. 4) were adiabatically adjusted to the surface pressure at the tower (a PROFS procedure) to remove topographic height variations from the resulting temperature analyses. This gave potential temperature analyses reduced to the ~850 mb pressure level. The front entered the network shortly after 1800 GMT (Fig. 4a) and passed rapidly southward (Figs. 4b, c and d) to the southern limit of the network by 2100 GMT with a speed of ~15 m s^{-1}. The westward movement of the front and cold air was impeded by the blocking action of the steep slope of the mountain lee. The sharpness of the temperature gradient and wind direction shift between Platteville (PTL) and Loveland (LVE), Colorado, at 1910 GMT (Fig. 4b) gave the first indication of the narrowness of the front. The discrepancy

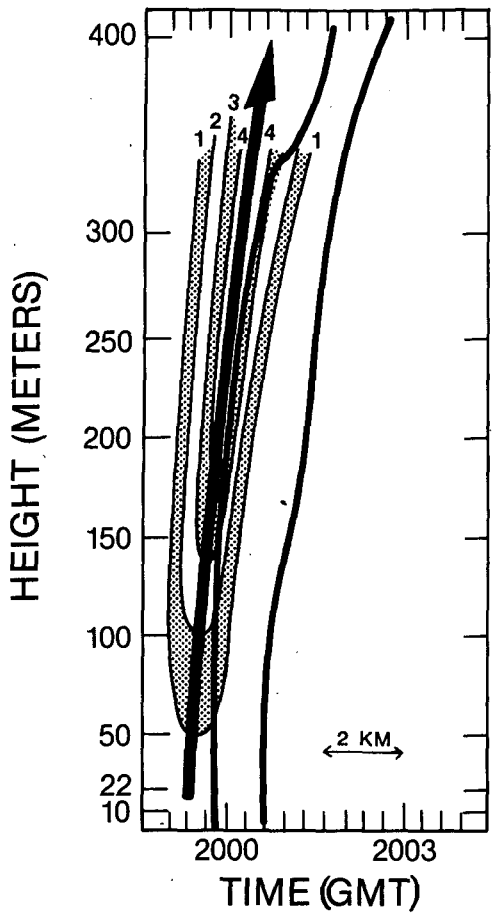

FIG. 8. Vertical motion (m s^{-1}) at the leading edge of the front shown in Fig. 7. Frontal boundaries from Fig. 7, heavy solid lines.

between the frontal analyses shown in Figs. 3 and 4d illustrates the value of regional networks in describing mesoscale frontal phenomena.

The BAO tower measurements revealed several dramatic characteristics of the front, which are shown in the temperature and wind speed traces from the 250 and 50 m levels of the tower (Fig. 5). The 50 m traces contained an 8°C temperature drop and a coincident 7 m s^{-1} wind speed surge and cyclonic shear within 1 min as the front passed shortly after 2000 GMT. The frontal convergence and vorticity were coincident as was the case described in Shapiro (1984). Orlanski and Ross (1984) have suggested that frontal convergence and vorticity can decouple with the convergence leading the vorticity. For a frontal speed of 15 m s^{-1} as taken from Fig. 4, the 1 min interval of frontal passage translates to a micro-α scale frontal width of 900 m. The wind direction (not shown) shifted by 90° (315° to 045°) during passage. A second wind speed surge (from 10 up to 17 m s^{-1}) occurred between 2005 and 2008 GMT, 4 min after frontal passage at 50 m. Similar changes in wind and temperature were recorded at the 10, 22 and 100 m tower levels. The temperature traces at 150 m, and above, contained features not evident at lower levels. This is shown in the 250 m temperature trace (Fig. 5), where the front passed in two distinct temperature drops between 2000 and 2002 GMT, with a slight temperature rise between the two, after which the temperature rose by 3°C at 2005 GMT, and then cooled with turbulent undulations of 2°C amplitude.

The acoustic profiler record (Fig. 6) provided the necessary information for interpreting the unusual undulations in the frontal traces measured at the tower. Figure 6 represents the contouring of the maximum echo intensity which appeared on the acoustic profiler records. The acoustic profiler receives enhanced returns from elevated turbulent layers, especially those with strong refractive index discontinuities like those found at fronts, stable layers and elevated inversions. The acoustic record showed frontal passage at 2000 GMT and the rapid rise in altitude of the front into an elevated 550 m head. The frontal head was followed by a turbulent wake that lowered to below 150 m after which the front rose to above 300 m. This represents a remotely sensed record of the hydraulic head at the leading edge of the front. The acoustic record below 300 m is similar in structure with the observed oscillations in potential temperature measured at the tower and analyzed in Fig. 7.

The BAO tower and acoustic sounder observations were composited into an analysis of the front. The acoustic record was used to specify the vertical excursion of the frontal head above the 300 m limit of the tower. The resulting potential temperature analysis (Fig. 7) shows the arrival of the elevated frontal head 3 min after frontal passage, and the turbulent wake that followed in its lee. The leading edge of the front passed the tower in two distinct surges, with the major portion of the wind direction switch occurring within the first packet of isentropes. The analysis of the total horizontal wind speed showed surges to 18 m s^{-1} at the 150 m level in the near-adiabatic layer behind and beneath the turbulent wake. This speed surge beneath the turbulent wake is outlined by the stippled 12–14 m s^{-1} isotach interval (Fig. 7). Note the in-phase relationship between the undulations in potential temperature and wind speed in the wake between 2005 and 2012 GMT (Fig. 7) as the vertical motions of trapped gravity waves and shear instability turbulence simultaneously raised and lowered the isopleths of temperature and velocity within the frontal layer. Wind speeds in the adiabatic layer beneath the frontal head averaged 9 m s^{-1} between 2001 and 2005 GMT.

The vertical velocity measurements from the tower sonic anemometers contained strong ascending motions at the leading edge of the frontal head (Fig. 8), with the maximum upward motion of 4.5 m s^{-1} at

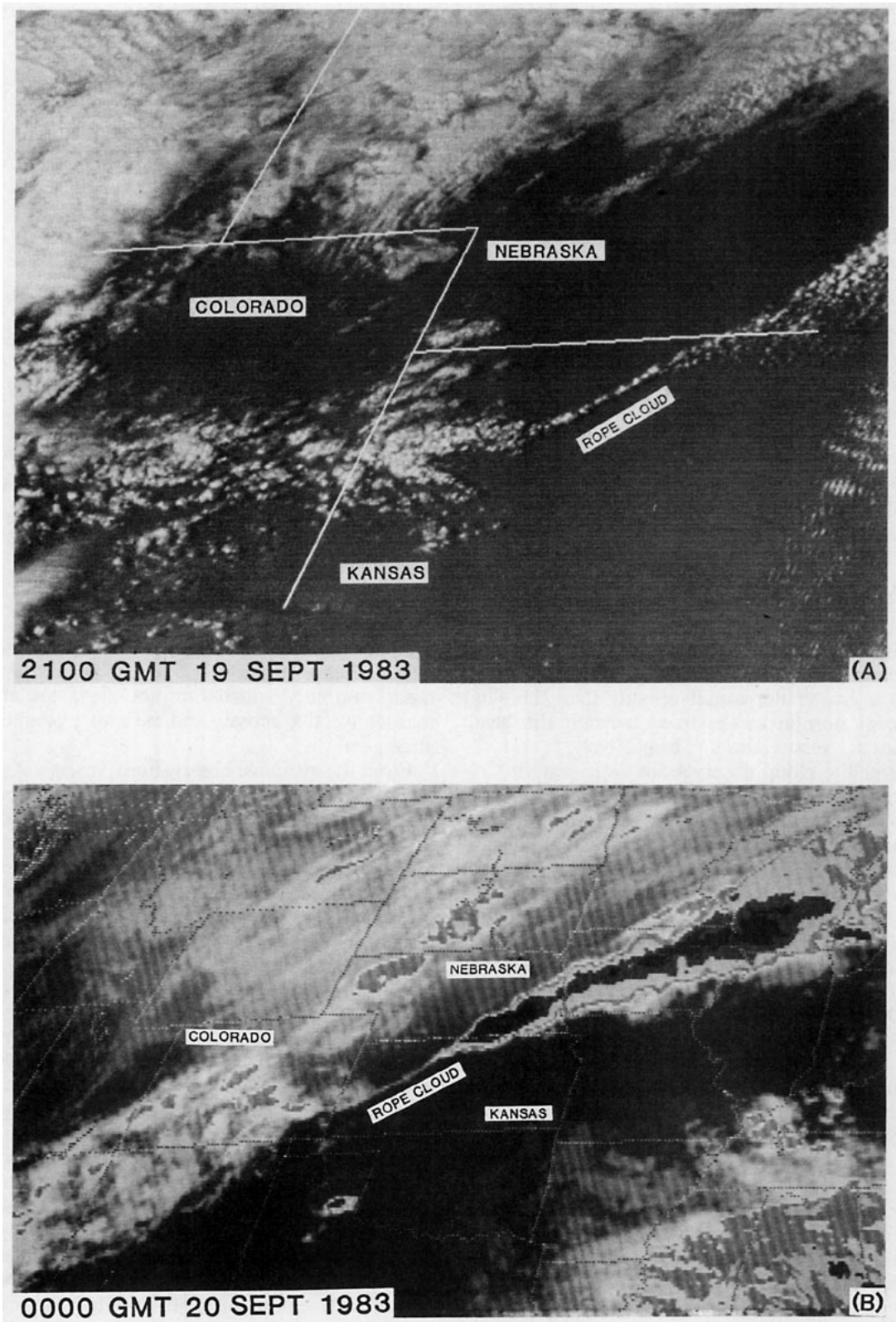

FIG. 9. (a) NOAA/GOES-5 satellite visible image at 2100 GMT 19 September 1983. (b) NOAA/GOES-5 IR image at 0000 GMT 20 September 1983. Contour grey scale is from the enhancement (MB) curve of Clark (1983).

the 300 m level. The magnitude and distribution of this ascent is similar to that of the previously described front (Fig. 2). There were no observations of the vertical extent of the ascent plume nor its maximum value. The vertical motions following frontal head passage were quite chaotic (especially within the turbulent wake), but lesser in magnitude (<2.5 m s^{-1}), and were not included in the analysis of Fig. 8.

After Carbone (1982), we calculated the speed of the leading edge of the density current, V, from the expression (von Kármán, 1940)

$$V = \left(K^2 g h \frac{T_1 - T_2}{T_2}\right)^{1/2} \quad (1)$$

where T_1 and T_2 are the virtual temperatures of the lighter and denser air masses, respectively, g is gravity, h the depth of the layer behind the head and K^2 = 1.4. For this case, h was determined from the acoustic record which showed the continued thickening of the post frontal cold boundary layer (beneath the frontal inversion) to ~500 m at 20 min after frontal head passage (not shown in Fig. 6). For the present case, h = 500 m, T_1 = 298 K, T_2 = 290 K and K^2 = 1.4 and the resulting speed of the density current (frontal head) was 14 m s^{-1}, in close agreement with the previously discussed frontal motion taken from Fig. 4. It should be noted that the leading edge of the density current and its hydraulic head propagated at a greater horizontal velocity than the wind component normal to the front beneath the head; i.e., 15 m s^{-1} versus 9 m s^{-1}, respectively.

The satellite cloud observations over eastern Colorado did not exhibit sufficient structure to permit easy frontal identification from a single image. However, the animated McIDAS video loop with 30 min temporal resolution did show a narrow band of enhanced cloudiness imbedded with a broken cumulus layer which surged southward with the leading edge of the front over the PROFS mesonetwork (Fig. 4). This surging band was suspected to result from strong ascent (Fig. 8) at the frontal head. Figure 9a shows the NOAA/GOES-5 satellite visible image at 2100 GMT 19 September 1983. Of specific interest is the narrow "rope" cloud line that extended northeastward across northwestern Kansas at the leading edge of the front shown in Fig. 3. The transverse scale of the thin cloud (~3 km) is similar to that of the ascending plume at the leading edge of the frontal head shown in Figs. 2 and 8. At 0000 GMT, the rope cloud was also present in the satellite infrared imagery (Fig. 9b) and extended diagonally across northwestern Kansas. The cold (darker) upper-level cloud structure which extends northwestward from the rope cloud (Fig. 9b) is the outflow from the mesoconvective activity that erupted as the front intercepted the region of enhanced low-level moisture over eastern Nebraska and Iowa. The gray-scale contours for Fig. 9 are taken from the Enhancement (MB) curve as described in Clark (1983). Figure 10 shows the 2035 GMT 19 September radar summary which outlines the areas of severe mesoconvective activity and the severe weather watch area.

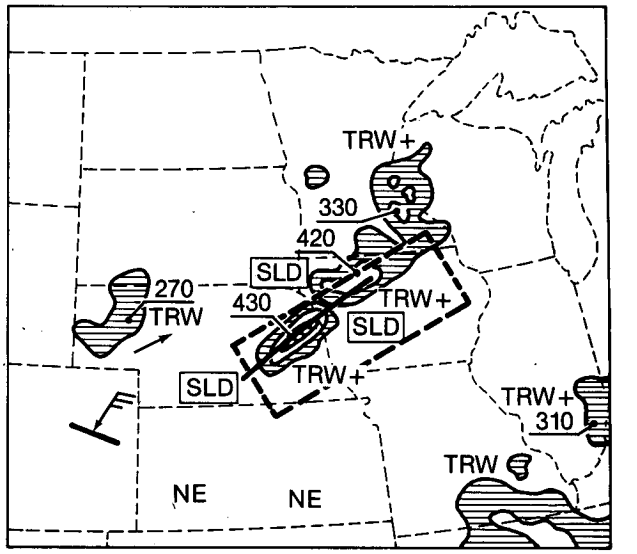

FIG. 10. National Weather Service radar summary at 2100 GMT 19 September 1983; TRW; thunderstorm; SLD, solid, NE, no echo. Echo height indicated in hundreds of feet.

From the available observations, it was not possible to provide conclusive evidence that the rope cloud (Fig. 9) was the signature of mesoscale ascent at the eastern extension of the frontal hydraulic head (Figs. 6–8). However, the barograph traces at surface stations within Nebraska, Colorado and Kansas showed strong pressure rise (surges) at time of frontal passage. An isochrone analysis of the time of surge passage for the 19 September 1983 front is shown in Fig. 11 along with some selected pressure traces. The pressure surge at the tower was coincident with the frontal passage. The position of the surge at 2100 and 0000 GMT (Fig. 11) coincides closely with the 2100 GMT and 0000 GMT position of the rope cloud in the satellite images (Fig. 9). It should be noted that standard National Weather Service (NWS) barographs have damping mechanisms which inhibit their ability to resolve hydraulic-head pressure perturbations whose time-scale of passage is tens of seconds or less.

On the following day, at 1800 GMT 20 September 1983, the front extended from Arkansas across Texas (Fig. 12) with a narrow rope cloud line of enhanced cumulus development at its leading edge (Fig. 13a). By 2000 GMT (Fig. 13b), the cloud line of Fig. 13 developed into a squall line with embedded cumulonimbus cellular "popcorn" structure. The above two-

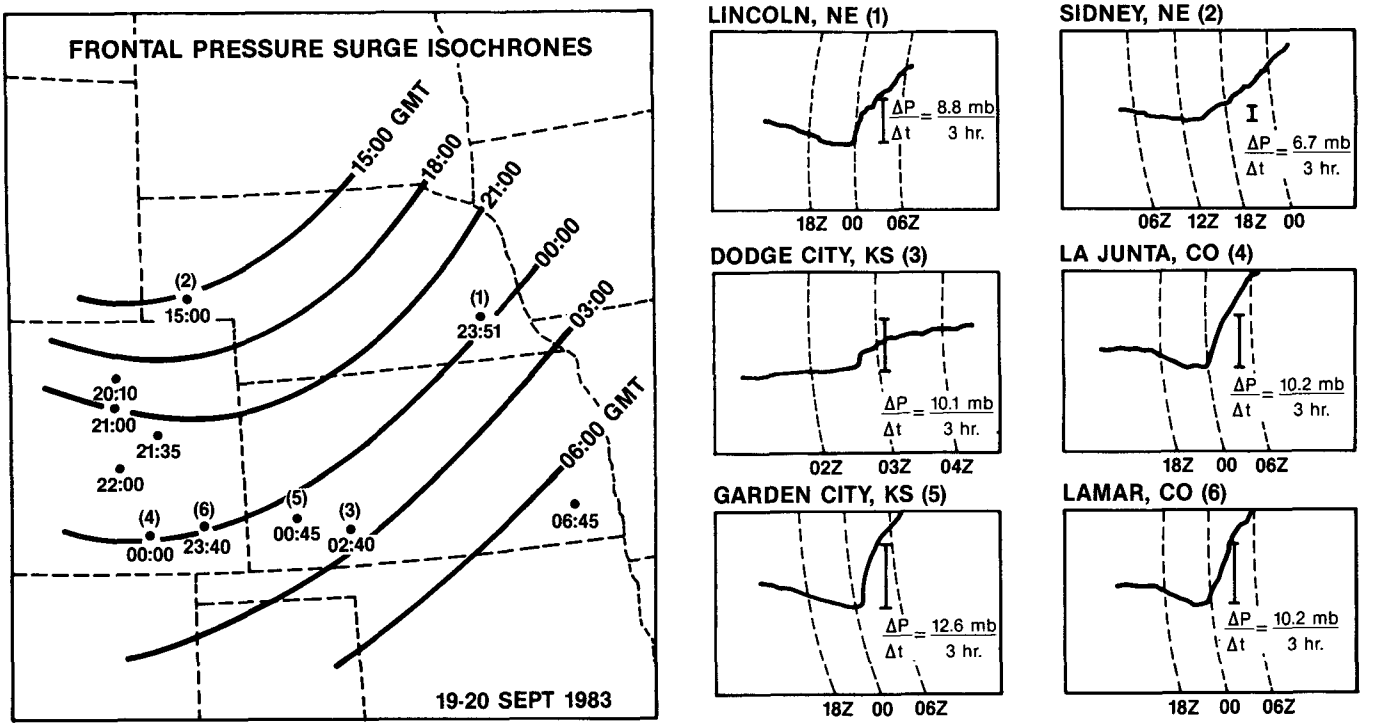

FIG. 11. Frontal pressure surge, 19–20 September 1983. (a) Isochrones (hr) of pressure surge and plotted times (GMT) of surge onset at selected stations. (b) Barograph traces from numbered stations in (a). Three-hourly pressure tendencies [mb (3 h)$^{-1}$] for the 3 h interval following surge onset.

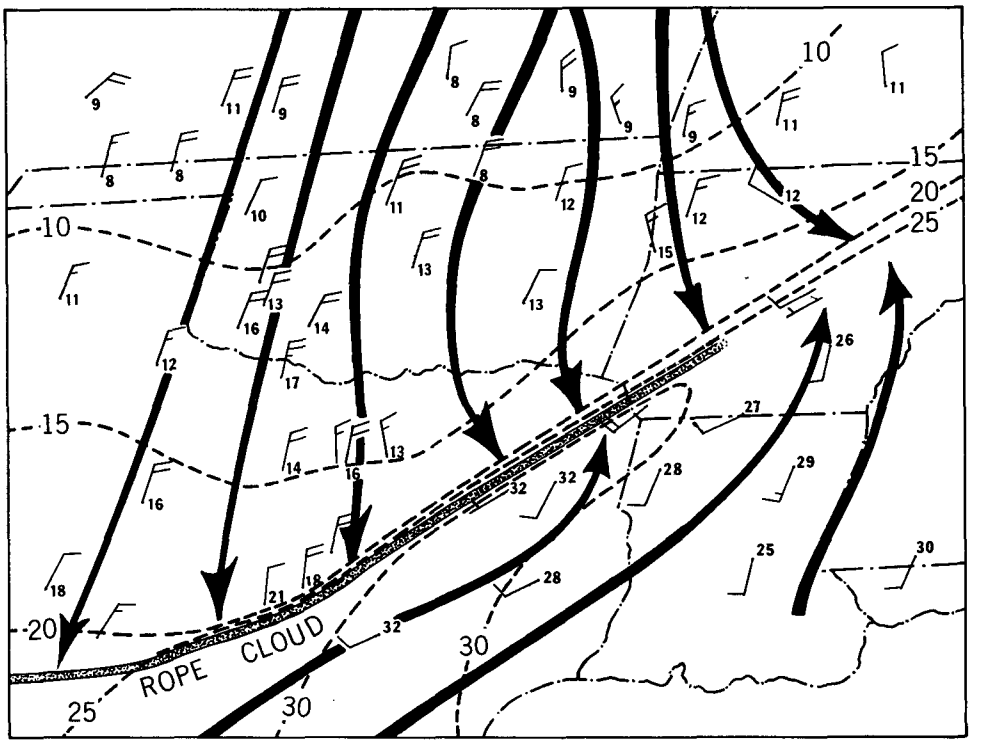

FIG. 12. Surface streamlines (solid lines) and temperature (°C, dashed lines) at 1800 GMT 20 September 1983. Flags and barbs, as indicated in Fig. 3; rope cloud of Fig. 13, stippled line.

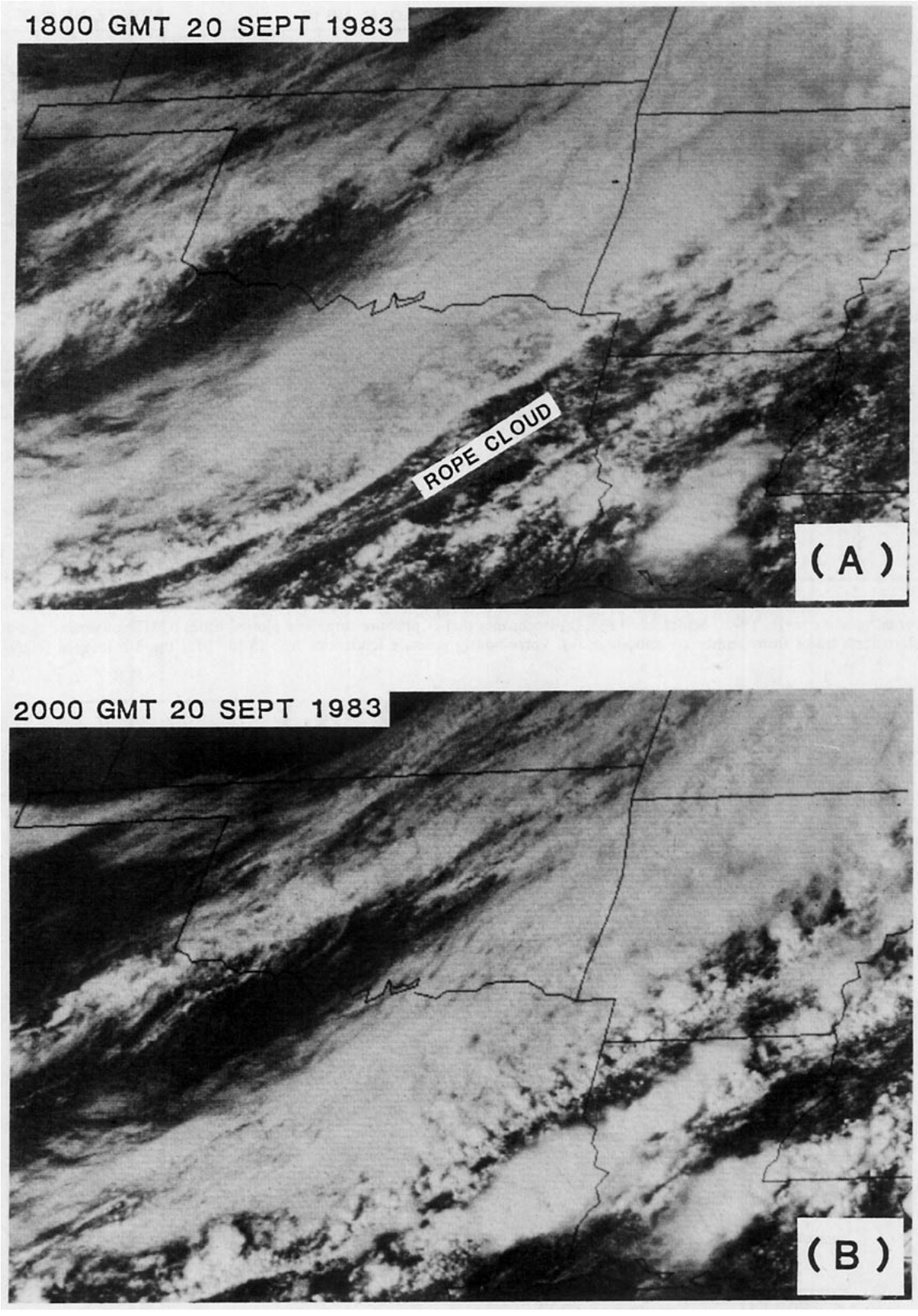

FIG. 13. NOAA/GOES-5 satellite visible images at (a) 1800 and (b) 2000 GMT 20 September 1983. Rope cloud of (a), same as indicated on Fig. 12.

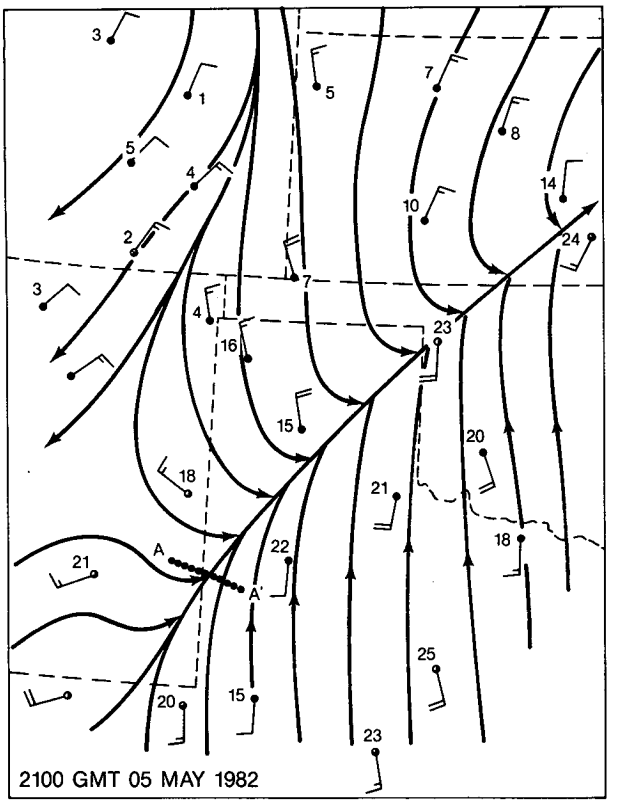

FIG. 14. Surface streamlines at 2100 GMT 5 May 1982. Flags and barbs, as in Fig. 3. Line AA', flight track of NCAR Sabreliner in Fig. 15.

day sequence represents our first example which *suggests* that micro-α scale ascent at the leading edge of initially dry surface fronts may be an important component in the life cycle of mesoconvective weather systems.

4. The surface cold front of 5 May 1982

Our second set of observations of micro-α scale frontal contraction was measured with the NCAR Sabreliner research aircraft. The synoptic setting for this case was one in which a cold front propagated southeastward in the lee of the Rocky Mountains. By 1800 GMT 5 May 1982, the front was oriented northeast to southwest through Oklahoma, the Texas panhandle and southeastern New Mexico (Fig. 14). The first of three frontal penetrations was made at 887 mb over west Texas between Roswell, New Mexico, and Abilene, Texas. Additional penetrations were made at 857 and 911 mb, after which the Sabreliner flew to the east, landing at Abilene at ~2000 GMT. Figure 15 presents the analysis of the flight observations for this case. The potential temperature analysis (Fig. 15a) shows the 4 K temperature gradient in ~1 km horizontal distance across the front. A dramatic shift in wind direction occurred at each of the three flight levels (Fig. 15a) when the Sabreliner penetrated the front. Note that at the 857 mb flight level, the wind was northwesterly in the cold air beneath the head and then returned to southwesterly flow in the warmer air to the west.

The equivalent potential temperature analysis (which shows the combined effect of temperature and moisture discontinuities) and gust probe vertical velocity measurements (Fig. 15b) provided further documentation for the structure of the frontal head. Ascending vertical velocities exceeding 5 m s^{-1} were measured just in advance of the frontal head, in agreement with the previously described cases (Sections 1 and 3). The leading edge of the front possessed the character of the hydraulic frontal head described in Section 3. The observations of the microscale frontal structure (Fig. 15) were taken just prior to the onset of severe mesoconvective activity. All flight legs of Fig. 15 were made below cloud base and were flown under Visual Flight Regulation (VFR) conditions without entering precipitation. Shortly after the Sabreliner's landing at Abilene, tornadoes were reported in association with thunderstorms near the front. The extent of the mesoconvection that erupted as the front entered the Gulf of Mexico moisture of >11 g kg^{-1} mixing ratio over central Texas is shown in the NWS radar summary for 0135 GMT 6 May 1982 in Fig. 16. Though this front exhibited micro-α scale head structure, the satellite imagery did not contain a narrow rope cloud as a precursor to the mesoconvective development.

5. The surface cold front of 9–10 June 1984

There are numerous examples when visible satellite imagery shows the cloud signature associated with micro-α to meso-γ (0.2 to 20 km) ascent at the leading edge of surface fronts (e.g., Shapiro, 1982; Koch, 1984) prior to mesoconvective outbreaks. The narrowness of these cloud lines suggests that they are associated with fronts that have contracted down as narrow as the microscale. The rope cloud can form in the narrow ascending plume within the upward branch of meso-β secondary circulations (Koch, 1984), or be forced by hydraulic heads at the leading edge of frontal density currents (Figs. 2 and 8). The following example illustrates the development of mesoconvective activity along a pre-existing frontal rope cloud.

On the afternoon of 9 June 1984, a cold front to the lee of the Rocky Mountains was situated across eastern Nebraska, eastern Kansas and western Oklahoma (Fig. 17). By 1800 GMT, mesoconvective activity was occurring along the northern segment of the front over northeastern Kansas and southeastern Nebraska (Fig. 18a and 19a). Figure 18 shows the NOAA/GOES-5 visible imagery at hourly intervals between 1800 and 2100 GMT 9 June 1984. At 1800

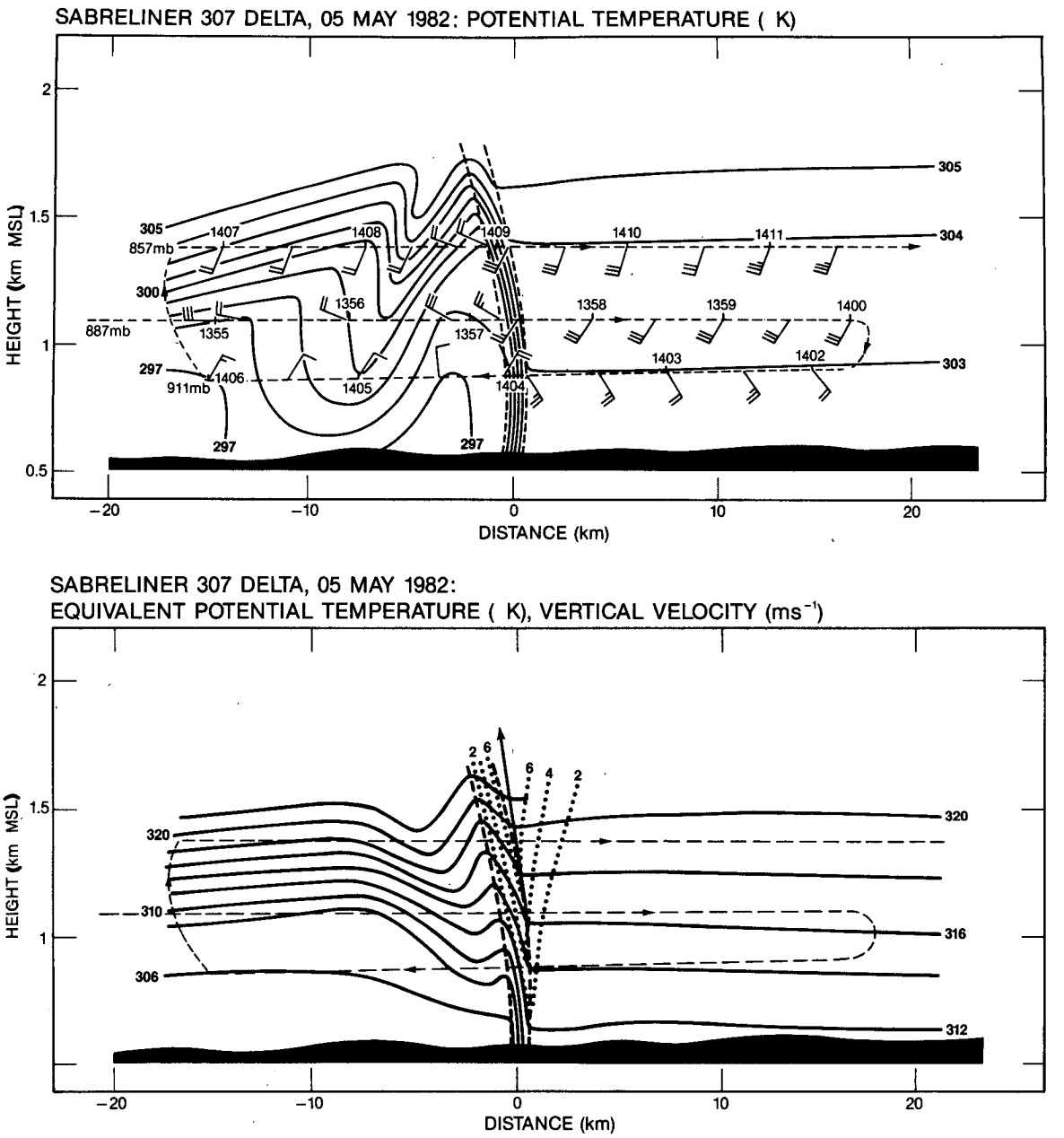

FIG. 15. Analysis of NCAR Sabreliner aircraft measurements of a microscale cold front on 5 May 1982. Sabreliner flight track, long dashed line with MST time hacks (MST = GMT + 7 h). (a) Potential temperature (K, solid lines); selected wind vectors, flags and barbs as in Fig. 3. (b) Equivalent potential temperature (K, solid lines); vertical velocity (m s^{-1}, short dashed lines).

GMT (Fig. 18a) a thin line of enhanced cumulus development extended from central Kansas to the Texas panhandle along the leading edge of the cold front. This rope cloud line marked the discontinuity between the cool, dry northwesterly flow to the northwest and the warmer moist southerly flow from off the Gulf of Mexico. Note the 40-km wavelength cloud lines embedded in the stratocumulus layer (Fig. 18a, central Oklahoma) in advance of the front. These cloud lines are probably the result of vertical circulations in the pre-frontal boundary layer, whose orientation is transverse to the boundary layer vertical wind shear vector. Reference to Fig. 17 shows that the rope cloud (Fig. 18b) is situated at the frontal wind shift between the two surface network stations at Wichita, Kansas (indicated by dashed circle). By 1900 GMT (Fig. 18b), the rope cloud began to broaden in response to the development of the cu-

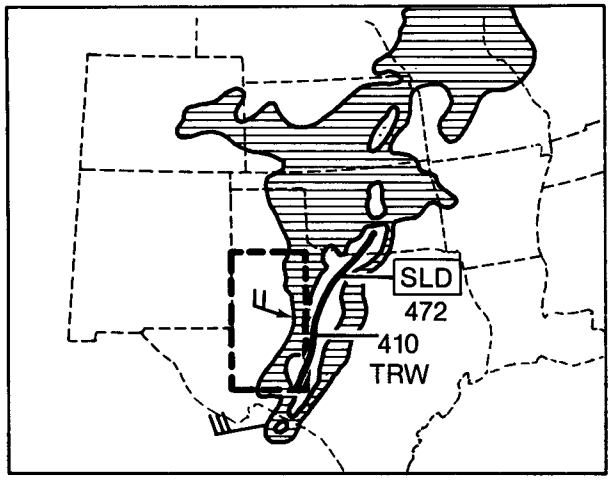

FIG. 16. National Weather Service radar summary at 0135 GMT 6 May 1982. Plotting convention as in Fig. 11.

mulus activity along the front. At 2000 GMT (Fig. 18c), the anvil outflow signature of cumulonimbus had erupted along the front in southern Kansas and northern Oklahoma. The final image (Fig. 18d) shows the fully developed cirrus outflow along the 500 km long squall line, with new convection breaking out at the southern remnant of the rope cloud. The NOAA/GOES-5 infrared images at 2 h intervals, from 1800 GMT 9 June to 0400 GMT 10 June 1984 are shown in Fig. 19. These images show the horizontal and vertical development of the mesoconvective system (MCS) cirrus anvil outflow. The visible and infrared satellite images of Figs. 18 and 19 suggest the presence of micro-α scale ascent as a precursor to the outbreak of the mesoconvective activity on this day. Unfortunately, there were no surface temperature or wind observations to document the coincidence of this rope cloud with frontal hydraulic head structure of the type described in Sections 1, 3 and 4.

6. Summary and discussion

The present study has shown additional documentation for the contraction of surface frontal gradients from the mesoscale down to the microscale, in the absence of convective precipitation. Of special notice are the observations of the elevated hydraulic head at the leading edge of the front and the several meter per second ascent in advance of the head as it propagates into the prefrontal warm air. The fronts described herein have the structural characteristics of classical density current flows cited in the introduction of this article.

It is interesting to note that we have come full circle in our interpretations, having put aside the early near zero-order discontinuity frontal models only to find such structure almost a century later using "modern" instrumentation. The fast response of the platinum wire temperature sensors on the BAO tower recorded frontal passages in time intervals as small as 10 s, giving the 170 m scale for the front shown in Fig. 1. The quartz thermistors on the same tower, similar to those used for continuous temperature records at the PROFS mesonetwork stations and NWS stations, required up to 6 min to record the same temperature drop as the platinum wires. The near zero-order frontal discontinuity concepts were undoubtedly based upon the fast response of the human skin (and mercury thermometers) as researchers stood in the elements to directly sense the wind and temperature changes during frontal passages. The conceptual models of fronts have evolved in response to the sensitivity and spatial resolution of the observing networks. Sanders (1955) suspected that the surface cold front he observed in a meso-β scale ($\sim$100 km) network was only "a few kilometers wide at the surface," but because the spatial resolution and hourly reporting frequency of the network he was unable to resolve its true time or space scale.

Fronts and their associated vertical circulations have long been recognized as a mechanism for lifting moist air to its level of free convection and initiating the release of potential instability through deep mesoconvective cloud systems. An alternative hypothesis for triggering prefrontal thunderstorms was proposed

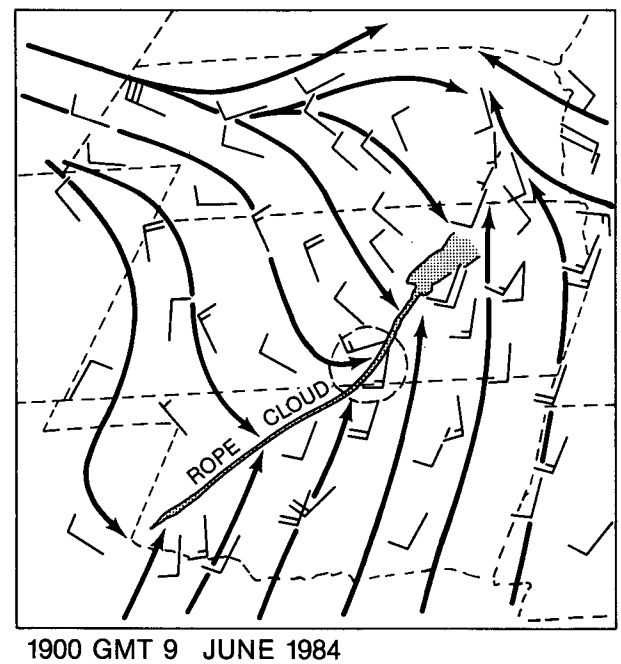

FIG. 17. Surface streamline analysis at 1900 GMT 9 June 1984. Rope cloud, (stippled) is from Fig. 18b. Flags and barbs as in Fig. 3.

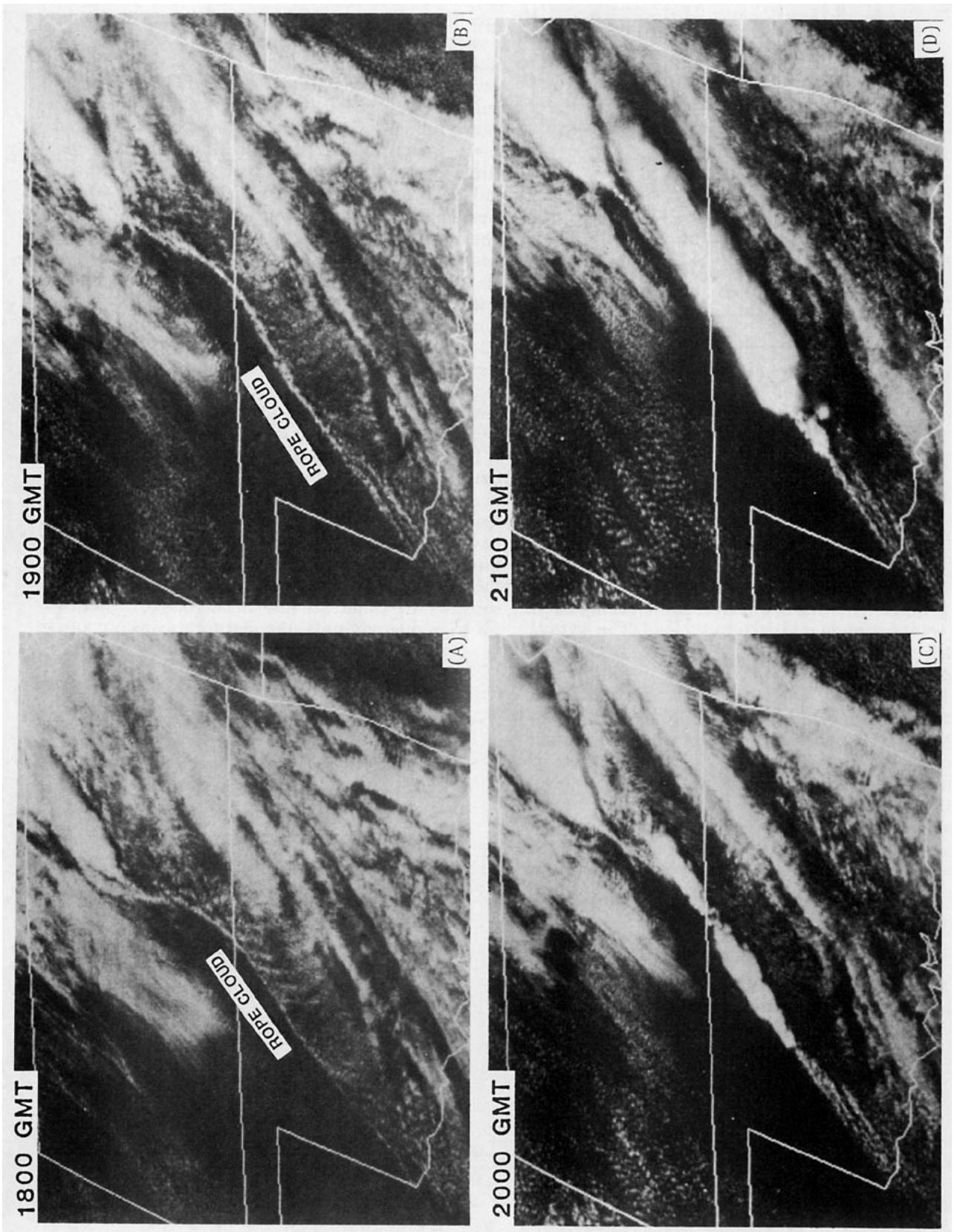

FIG. 18. NOAA/GOES-5 satellite visible cloud images at 1800 GMT, 1900 GMT, 2000 GMT and 2100 GMT 9 June 1984 as prepared on the University of Wisconsin McIDAS interactive meteorological graphics system.

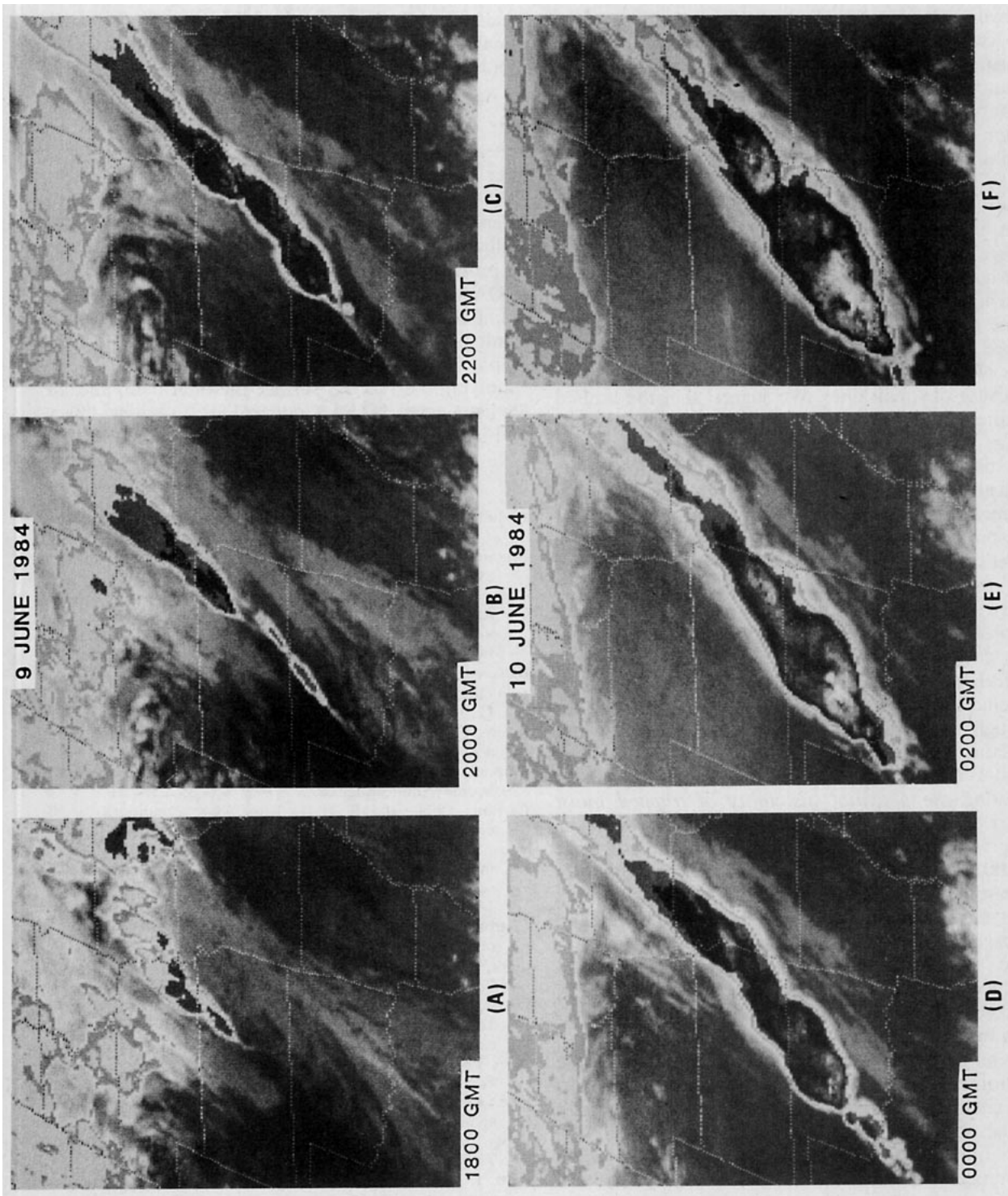

FIG. 19. NOAA/GOES-5 satellite infrared cloud images at 2 h intervals between 1800 GMT 9 June 1984 and 0400 GMT 10 June 1984, (a) through (f), as transmitted by the National Weather Service via Laser Fax. Contour grey scale is as indicated in Fig. 9b.

in the theoretical treatments of Freeman (1948) and Abdullah (1949), with extensive observational documentation by Tepper (1950). These studies proposed that frontal and prefrontal squall lines were initiated by hydraulic pressure waves or "jumps" formed by the accelerated motion of fronts. On occasion these pressure jumps were thought to propagate out in advance of the triggering front. The documentation by Tepper (1950) was taken from an automatic 55-station microbarograph, wind and temperature observing network with ~3 km spatial resolution of the observing stations. Newton (1950) questioned the importance of the pressure jump triggering mechanism, stating that the vertical excursions in trapped surface moisture layers caused by the jumps and their propagating gravity waves would not be sufficient to raise air parcels to their level of free convection, and hence produce squall line convection. Fujita (1955) argued and presented evidence that the pressure jump lines of Tepper (1950) were the result of, rather than the cause of squall lines. We suggest that the limited acceptance of nonhydrostatic, micro-α scale phenomena as an initiation mechanism for mesoconvective systems was due to the lack of documentation of the vertical structure of the pressure jump lines. It is only recently that instrumented towers and research aircraft have provided some corroborating evidence for density current (hydraulic head) characteristics of surface cold fronts, thunderstorm outflows and sea-breeze fronts. The present study has shown examples where *nonprecipitating fronts have assumed the characteristics of density-current flows.* The large ascending vertical motions (~5 m s^{-1}) at the frontal head are of sufficient magnitude to lift potentially unstable air through the trapping "lid" inversions (Carlson and Ludlam, 1968; Carlson *et al.*, 1983) which often cap moist surface layers. *The frontal head is capable of releasing the potential instability of trapped moist layers on time scales of minutes rather than hours* as required for the 20 cm s^{-1} lifting of meso-β scale (~100 km) frontal vertical circulations. It is not unreasonable to consider the possibility that the frontal head may separate itself from its parent front and propagate out in advance of the front as a solitary wave (Abdullah, 1949). The separation process could produce prefrontal pressure waves (as in Tepper, 1950; Uccellini, 1975) and initiate precipitation systems in the prefrontal environment.

It remains for future research to 1) establish the relationship between frontal deformations, their vertical circulations, and surface boundary layer processes in the scale collapse of frontal gradients and the formation of frontal hydraulic heads, 2) derive the theoretical treatments which describe the transition from geostrophic-momentum (semigeostrophic) dynamics over to nonhydrostatic, primitive equation dynamics as frontal gradients transcend the meso-α scale down to the micro-α scale and 3) carry out further field experiments with research aircraft, Doppler lidars, Doppler radars and fast response (~1 s) surface based instruments so as to clearly establish the role and representativeness of the hydraulic frontal heads, described herein, in initiating the formation of narrow rope cloud lines and severe mesoconvective weather systems.

Acknowledgments. The authors express their gratitude to Dr. Byron Phillips (Director of the NCAR Research Aviation Facility) for providing the Sabreliner aircraft used in this study, Dr. John Gaynor (NOAA/WPL) for assisting in accessing and the interpretation of the BAO tower observations, Dr. William Neff (NOAA/WPL) for furnishing the acoustic profiler records of frontal passages, Denis Rodgers (NOAA/ERL Environmental Studies Group) for providing the NOAA/GOES-5 satellite IR images, Robert Zamora (NOAA/WPL) for his analysis of the barograph traces, Dr. Thomas Schlatter (PROFS) for supplying the PROFS surface mesonet data, and Dr. Daniel Keyser (NASA/Goddard) for his critical review and helpful comments.

REFERENCES

Abdullah, A. J., 1949: Cyclogenesis by a purely mechanical process. *J. Meteor.*, **6**, 86–97.

Bergeron, T., 1928: Über die dreidimensional verknüpfende Wetteranalyse (I). *Geofys. Publ.*, **5**(6), 1–111.

——, 1959: Methods in scientific weather analysis and forecasting. An outline in the history of ideas and hints at a program. *The Atmosphere and the Sea in Motion,* B. Bolin, Ed., Rockefeller Institute Press, 440–474.

Bjerknes, J., and E. Palmén, 1937: Investigations of selected European cyclones by means of serial ascents. *Geofys. Publ.*, **12**, 1–61.

Brown, E. H., and F. F. Hall, Jr., 1978: Advances in atmospheric acoustics. *Rev. Geophys. Space. Phys.*, **16**, 47–110.

Carbone, R. E., 1982: A severe frontal rainband. Part I: Stormwide hydrodynamic structure. *J. Atmos. Sci.*, **39**, 258–279.

Carlson, T. N., and F. H. Ludlam, 1968: Conditions for the occurrence of severe local storms. *Tellus,* **20**, 203–226.

——, S. G. Benjamin, G. S. Forbes and Y. F. Li, 1983: Elevated mixed layers in the regional severe storm environment: Conceptual model and case studies. *Mon. Wea. Rev.*, **111**, 1453–1473.

Charba, J., 1974: Application of a gravity current model to analysis of squall-line gust front. *Mon. Wea. Rev.*, **102**, 140–156.

Clark, J. Dane, 1983: The GOES User's Guide. U.S. Dept. of Commerce, NOAA/NESDIS, Washington, DC.

Eliassen, A., 1959: On the formation of fronts in the atmosphere. *The Atmosphere and the Sea in Motion,* B. Bolin, Ed., Rockefeller Institute Press, 277–287.

——, 1962: On the vertical circulation in frontal zones. *Geofys. Publ.*, **24**, 147–160.

Freeman, J. C., Jr., 1948: An analogy between equatorial easterlies and supersonic gas flow. *J. Meteor.*, **5**, 138–146.

Fujita, T., 1955: Results of detailed synoptic studies of squall lines. *Tellus,* **7**, 405–436.

Fultz, D., 1951: Experimental analogies to atmospheric motions. *Compendium of Meteorology,* T. F. Malone, Ed., Amer. Meteor. Soc., 1235–1248.

Goff, R. C., 1976: Vertical structure of thunderstorm outflows. *Mon. Wea. Rev.*, **104**, 1429–1440.

Hobbs, P. V., and P. O. G. Persson, 1982: The mesoscale and

microscale structure and organization of clouds and precipitation in midlatitude cyclones. Part V: The substructure of narrow cold-frontal rainbands. *J. Atmos. Sci.*, **39**, 280–295.

Hoskins, B. J., and F. P. Bretherton, 1972: Atmospheric frontogenesis models: Mathematical formulation and solution. *J. Atmos. Sci.*, **29**, 11–37.

Kaimal, J. C., and J. E. Gaynor, 1983: The Boulder Atmospheric Observatory. *J. Appl. Meteor.*, **22**, 864–880.

Keyser, D., and R. A. Anthes, 1982: The influence of planetary boundary layer physics on frontal structure in the Hoskins-Bretherton horizontal shear model. *J. Atmos. Sci.*, **39**, 1783–1802.

Koch, S. E., 1984: The role of an apparent mesoscale frontogenetic circulation in squall line initiation. *Mon. Wea. Rev.*, **112**, 2090–2111.

Margules, M., 1906: Über temperatursch-ichtung in stationar bewegter und ruhender luft. *Hann-Baud. Meteor.*, **2**, 245–254.

Matthews, D. A., 1981: Observation of a cloud arc triggered by thunderstorm outflow. *Mon. Wea. Rev.*, **109**, 2140–2157.

Middleton, G. V., 1966: Experiments on density and turbidity currents. Part I: Motion of the head. *Can. J. Earth Sci.*, **3**, 523–546.

Mitchell, K. E., and J. B. Hovermale, 1977: A numerical investigation of the severe thunderstorm gust front. *Mon. Wea. Rev.*, **105**, 657–675.

Newton, C. W., 1950: Structure and mechanism of the prefrontal squall line. *J. Meteor.*, **7**, 210–222.

Orlanski, I., and B. B. Ross, 1984: The evolution of an observed cold front. Part II: Mesoscale dynamics. *J. Atmos. Sci.*, **41**, 1669–1703.

Petterssen, S., 1956: *Weather Analysis and Forecasting. Vol. 1, Motion and Motion Systems*, 2nd ed., McGraw-Hill, 428 pp.

Sanders, F., 1955: An investigation of the structure and dynamics of an intense surface frontal zone. *J. Meteor.*, **12**, 542–552.

Sawyer, J. S., 1956: The vertical circulation at meteorological fronts and its relation to frontogenesis. *Proc. Roy. Soc. London*, **A234**, 346–362.

Schmidt, W., 1913: Weitere versche uber den boenvorgang und das wegschaffen der bodeninversion. *Meteor. Z.*, **30**, 441–447.

Shapiro, M. A., 1981: Frontogenesis and geostrophically-forced secondary circulations in the vicinity of jet stream-frontal zone systems. *J. Atmos. Sci.*, **38**, 954–973.

——, 1982: Mesoscale weather systems of the central United States. CIRES/NOAA Tech. Rep., University of Colorado, Boulder, CO, 78 pp.

——, 1984: Meteorological tower measurements of a surface cold front. *Mon. Wea. Rev.*, **112**, 1634–1639.

Simpson, J. E., 1969: A comparison between laboratory and atmospheric density currents. *Quart. J. Roy. Meteor. Soc.*, **95**, 758–765.

——, 1972: Effects of the lower boundary on the head of a gravity current. *J. Fluid Mech.*, **53**, 759–768.

——, D. A. Mansfield and J. R. Milford, 1977: Inland penetration of sea-breeze fronts. *Quart. J. Roy. Meteor. Soc.*, **103**, 47–67.

Tepper, M., 1950: A proposed mechanism of squall lines: The pressure jump line. *J. Meteor.*, **7**, 21–29.

Uccellini, L. W., 1975: A case study of apparent gravity wave initiation of severe convective storms. *Mon. Wea. Rev.*, **103**, 497–513.

von Kármán, T., 1940: The engineer grapples with nonlinear problems. *Bull. Amer. Math. Soc.*, **46**, 615–623.

Wakimoto, R. M., 1982: Investigations of thunderstorm gust fronts with the use of radar and rawinsonde data. *Mon. Wea. Rev.*, **110**, 1060–1082.

Williams, R. T., 1967: Atmospheric frontogenesis: A numerical experiment. *J. Atmos. Sci.*, **24**, 627–641.